Prune as You Generate: Online Rollout Pruning for Faster and Better RLVR

Haobo Xu[1], **Sirui Chen**[1], **Ruizhong Qiu**[1], **Yuchen Yan**[2],
Chen Luo[2], **Monica Cheng**[2], **Jingrui He**[1], **Hanghang Tong**[1]
[1] University of Illinois at Urbana-Champaign [2] Amazon
{haoboxu, htong}@illinois.edu

Abstract

Reinforcement Learning with Verifiable Rewards (RLVR) has significantly advanced the reasoning capabilities of Large Language Models (LLMs). However, methods such as GRPO and DAPO suffer from substantial computational cost, since they rely on sampling many rollouts for each prompt. Moreover, in RLVR the relative advantage is often sparse: many samples become nearly all-correct or all-incorrect, yielding low within-group reward variance and thus weak learning signals. In this paper, we introduce ARRoL (**A**ccelerating **R**LV**R** via **o**nline Ro**L**lout Pruning), an online rollout pruning method that prunes rollouts during generation while explicitly steering the surviving ones more correctness-balanced to enhance learning signals. Specifically, ARRoL trains a lightweight quality head on-the-fly to predict the success probability of partial rollouts and uses it to make early pruning decisions. The learned quality head can further weigh candidates to improve inference accuracy during test-time scaling. To improve efficiency, we present a system design that prunes rollouts inside the inference engine and re-batches the remaining ones for log-probability computation and policy updates. Across GRPO and DAPO on Qwen-3 and LLaMA-3.2 models (1B-8B), ARRoL improves average accuracy by $+2.30$ to $+2.99$ while achieving up to $1.7\times$ training speedup, and yielding up to $+8.33$ additional gains in average accuracy in test-time scaling. The code is available at https://github.com/Hsu1023/ARRoL.

1 Introduction

Reasoning abilities of Large Language Models (LLMs) have recently gained great success in many domains such as mathematical problem solving and code generation (Jaech et al., 2024; Guo et al., 2025; Qiu et al., 2024b). Reinforcement Learning with Verifiable Rewards (RLVR) (Lambert et al., 2024; Yu et al., 2025c) as a critical technique plays an important role in enhancing reasoning ability of LLMs. A representative method is Group Relative Policy Optimization (GRPO) (Shao et al., 2024), which utilizes binary rewards such as correctness of a logical problem as learning signals and compute advantages within a group of rollouts per prompt. However, such methods are largely constrained by high computational cost (Xu et al., 2025; Lin et al., 2025b). During training, each prompt requires generating a large group of rollouts, which is computationally expensive, making training expensive and limiting the practicality of RLVR at scale.

To mitigate training cost, prior work has explored several directions. Some studies (Lin et al., 2025b; Xu et al., 2025) reduce the number of rollouts used for gradient estimation and policy updates. However, these methods typically manipulate rollouts at the post-generation level; therefore, they do not reduce rollout generation time, which can limit end-to-end speedups.

Other studies employ speculative decoding to accelerate rollout generation (He et al., 2025; Liu et al., 2025a), but they rely on historical sequences from previous epochs, which may vary and not suitable for commonly adopted small epochs settings. Moreover, they do not explicitly address a key issue in RLVR with binary rewards (0/1): when rewards within a group are highly imbalanced (e.g., mostly correct or mostly incorrect), the within-group reward diversity becomes low, leading to weak learning signals (Bae et al., 2025). In the extreme case where a group collapses to all 0s or all 1s, the group-normalized advantages can degenerate to zero, resulting in a vanishing policy gradient. This motivates a key question: *Can we reduce rollout cost while strengthening learning signals?*

To answer this question, we propose an online rollout pruning method that *carefully selects a correctness-balanced subset of rollouts for training during rollout generation* using a quality predictor. Concretely, we train a lightweight model head to

Proceedings of the 64th Annual Meeting of the Association for Computational Linguistics (Volume 1: Long Papers), pages 13876–13893

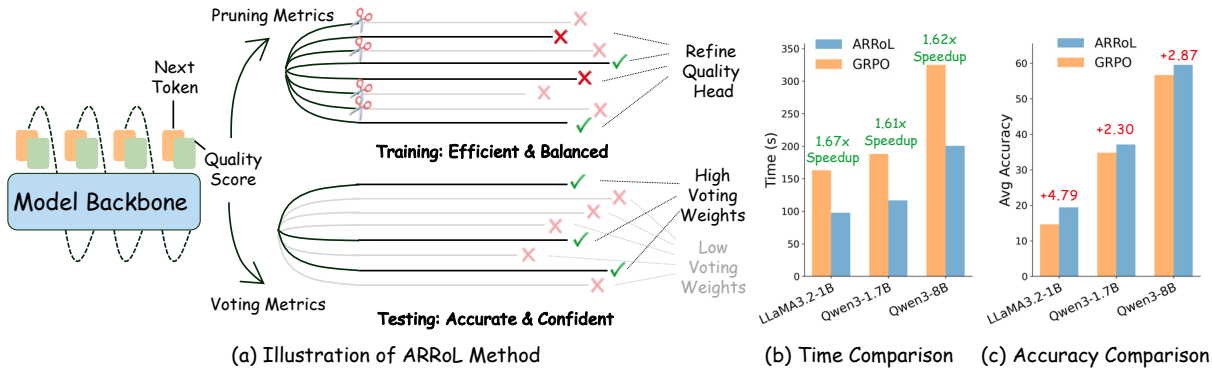

(a) Illustration of ARRoL Method (b) Time Comparison (c) Accuracy Comparison

Figure 1: **ARRoL overview and results.** (a) ARRoL uses a quality head to score partial rollouts, enabling early pruning for efficient and reward-balanced training, and the scores can also be used as voting weights for test-time scaling. (b) Wall-clock time comparison between ARRoL and GRPO across different model backbones, showing consistent speedups. (c) Accuracy comparison, where ARRoL improves average accuracy over GRPO.

score early-stage partial rollouts and map the score to an estimated success probability. The rollouts with final rewards can naturally be used as training data of rollouts, and it introduces negligible overhead.

We compare the quality scores with other heuristic metrics, such as DeepConf (Fu et al., 2025), and show that the scores generated by a learnable head are better than trace confidence across datasets, as the latter can be biased by patterns (e.g., reflections or formula-rich text) and may misalign with final correctness. Then, we prune the early-stage rollouts based on the quality scores to make the correctness of remaining rollouts more balanced. This yields a "less is more" effect: fewer rollouts continue to generate and involve in advantage computation, leading to less computation cost, while the remaining rollouts provide stronger learning signals due to improved balance. Furthermore, the learned quality head can naturally serve as a correctness predictor to weight candidates in *test-time scaling* to improve accuracy instead of naive majority vote.

To implement online pruning during generation and improve efficiency, we integrate pruning into a standard frontend–backend RL training architecture. The backend evaluates rollouts by the quality head at an early stage and immediately removes pruned sequences from the request pool, allowing the scheduler to reallocate freed capacity to other active sequences and reduce overall generation time. The frontend receives pruning masks, filters pruned rollouts, and re-batches the survivors for log-probability computation and optimization, leading to less computational cost as well.

In summary, our key contributions are as follows:

- **Online Rollout Pruning.** We propose an online, quality-head-guided rollout pruning strategy, ARRoL, which explicitly controls within-group reward balance while reducing compute, improving average accuracy of GRPO/DAPO training on Qwen-3 and LLaMA-3.2 models (1B-8B) by $+2.30$ to $+2.99$.
- **Test-time Scaling.** We leverage the trained quality head at inference time as voting weights for test-time scaling, improving final-answer aggregation, leading to $+8.33$ gains in average accuracy.
- **System Speedup.** We present a system design that realizes end-to-end speedups by pruning inside the generation backend and re-batching survivors in the frontend, achieving $1.6-1.7\times$ speedup.

2 Related Work

Efficient RLVR. Recent studies improve the efficiency of RLVR from different angles. Some modify rollout construction. For example, S-GRPO (Dai et al., 2025) derives a serial group of rollouts from a single trajectory, which may reduce trajectory diversity. Others leverage historical information. GRESO (Zheng et al., 2025) skips likely uninformative prompts before rollouts. RhymeRL (He et al., 2025) reuses historical rollout tokens by speculative decoding. However, these speedups rely on historical information

and can be limited in cold-start settings. Another line targets post-rollout optimization. CPPO (Lin et al., 2025b) prunes generated completions, and PODS (Xu et al., 2025) downsamples a large rollout pool, to accelerate the update phase. However, these methods do not directly reduce (and can even increase) token-generation cost during rollout. Several works target to accelerating rollout generation. Spec-RL (Liu et al., 2025a) and FastGRPO (Zhang et al., 2025a) employ speculative decoding, while FlashRL (Yao et al.) and QeRL (Huang et al., 2025) use low-precision/quantized rollouts to speed up token generation. In contrast, our method uses a lightweight logits-based probe to predict rollout utility online, enabling training-time pruning with controlled signal quality and a unified criterion that also supports test-time rollout filtering.

Test-time Scaling. Test-time scaling (TTS) improves reasoning performance by allocating additional compute at inference time without modifying model parameters. TTS is commonly categorized into sequential and parallel strategies. Sequential TTS increases compute along a single trajectory by extending reasoning process or revisiting the initial answer. For instance, s1 (Muennighoff et al., 2025) proposes budget forcing to terminate trajectories early or append double-check tokens to encourage rethinking. Other work studies the underthinking phenomenon and triggers deeper deliberation if necessary (Wang et al., 2025; Qiu et al., 2025b). In contrast, parallel TTS samples multiple trajectory candidates and aggregates them, including Self-Consistency (Wang et al., 2022; Cui et al., 2026), Best-of-N (Zhou et al., 2022; Qiu et al., 2025a), and adaptive voting (Snell et al., 2024). Recent studies further explore confidence-based TTS. DeepConf (Fu et al., 2025) uses log-probability-based confidence to prune low-confidence trajectories, while CGES (Aghazadeh et al., 2025) employs heuristic estimates or reward models to early-stop the sampling process. However, these heuristic confidence signals are typically not guaranteed to align with final-answer correctness, so their reliability may degrade under distribution shift or in out-of-domain settings.

3 Preliminaries

Trace Confidence. Recent work leverages model-internal uncertainty signals to evaluate the quality of an LLM-generated trace. Given the predicted token distribution $P_t(\cdot)$ at position t, token confidence is defined as $H_t = -\sum_{j=1}^{V} \log P_t(j)$, where V is the vocabulary size. Self-uncertainty (Kang et al., 2025) defines trace confidence as the average token confidence over the trace. DeepConf (Fu et al., 2025) further improves effectiveness and efficiency by computing window-level confidence. Specifically, it averages token uncertainty within a fixed-size sliding window w: $H_w = \frac{1}{|w|}\sum_{t\in w} H_t$, and then aggregates $\{H_w\}$ along the trace, e.g., using the minimum window value or the average of the bottom 10% windows as the trace-level score.

Reinforcement Learning with Verifiable Rewards (RLVR). Let the large language model be the policy π_θ that, given a prompt x, generates a rollout o that contains the reasoning trace and the final answer y. Assume a dataset $\mathcal{D} = \{(x_i, a_i)\}_{i=1}^{N}$, where a_i is the ground-truth answer to the prompt x_i. We define a verifiable reward $R(y_i, a_i) = \mathbb{1}[y_i \equiv a_i]$, where $\mathbb{1}[\cdot] \in \{0, 1\}$ is an indicator that evaluates whether y_i and a_i are equivalent, e.g., mathematically equivalent.

Group-Relative Policy Optimization (GRPO). GRPO (Shao et al., 2024) estimates advantages using the relative performance within a group of answers for the same prompt, without a value model. The objective is:

$$J(\theta) = \mathbb{E}_{(x,a)\sim\mathcal{D},\{o_i\}_{i=1}^{G}} \frac{1}{G}\sum_{i=1}^{G}\frac{1}{|o_i|}\sum_{t=1}^{|o_i|}\min[r_{i,t}A_i, \text{clip}(r_{i,t}, 1-\epsilon, 1+\epsilon)A_i] - \beta\cdot \text{KL}(\pi_\theta||\pi_{ref}),$$

where G is the group size, $r_{i,t} = \frac{\pi_\theta(o_{i,t}|o_{i,<t})}{\pi_{\text{ref}}(o_{i,t}|o_{i,<t})}$ is the importance ratio, and $A_i = \frac{R(y_i,a_i)-\text{mean}(\{R(y_j,a_j)\}_{j=1}^{G})}{\text{std}(\{R(y_j,a_j)\}_{j=1}^{G})}$ is the group-relative advantage. However, GRPO incurs substantial time cost because it must generate many rollouts per prompt and process them for log-probability computation and policy updates. Also, it can encounter sparse signal issue that rewards within a group are all 0/1 and group-normalized advantages become zero, leading to vanishing gradient.

4 Method

We introduce ARROL, a rollout pruning method to improve the efficiency of GRPO by balancing 0/1 rewards within each group. ARROL trains a lightweight model head, named quality head, to score partial rollouts, and uses these scores to select a balanced subset for training. The learned scores

can also be reused as voting weights at test time. We further present a system design that realizes the wall-clock speedup in practice.

4.1 Pruning Improves Sample Balance

GRPO suffers from sparse signals when the rewards are nearly all 0s or all 1s. Intuitively, a more balanced sample group will introduce larger variance within a group, leading to non-vanishing gradients. Also, if samples are balanced, we can avoid circumstances in which some groups are dominated by a few minority samples, leading to sparse and noisy learning signals. Recent studies (Bae et al., 2025) provide theoretical support that, under binary (0/1) rewards, the learning signal is proportional to the reward variance and is maximized when the pass ratio (i.e., the fraction of positive samples within a group) is close to 0.5, thereby improving the effectiveness of RL training. Based on this, letting the positive-sample ratio be ρ, we further show that rollout pruning can push the empirical ratio toward ρ (ideally $\rho = 0.5$), improving sample balance beyond its efficiency gains.

Lemma 4.1 (Existence of a Corrective Pruning)**.** *Consider a mini-batch of size G, each with a label $y_i \in \{0, 1\}$. We assume a fixed positive ratio $\rho \in [0, 1]$ and conditional independence given latent Bernoulli parameters: $Y_i|q_i^\star \sim$ Bernoulli$(q_i^\star)$. We define the batch mean $\mu^\star := \frac{1}{G}\sum_{i=1}^{G} q_i^\star$ and the pruned mean $\mu_{-j}^\star := \frac{1}{G-1}\sum_{i\neq j} q_i^\star$. If $\mu^\star > \rho$ and there exists an index j such that $q_j^\star > \mu^\star$, then pruning j strictly reduces the deviation to ρ:*

$$\left|\mu_{-j}^\star - \rho\right| < \left|\mu^\star - \rho\right|.$$

Symmetrically, if $\mu^\star < \rho$ and there exists j such that $q_j^\star < \mu^\star$, then the same conclusion holds.

Proof. Assume $\mu^\star > \rho$. If $q_j^\star > \mu^\star$, then

$$\mu_{-j}^\star - \mu^\star = \frac{G\mu^\star - q_j^\star}{G-1} - \mu^\star = \frac{\mu^\star - q_j^\star}{G-1} < 0,$$

so $\mu_{-j}^\star < \mu^\star$. Since $\rho < \mu^\star$, moving $\mu^\star$ downward moves it toward ρ, hence $|\mu_{-j}^\star - \rho| < |\mu^\star - \rho|$. The other case is symmetric. □

Theorem 4.2 (High-probability closeness to target ρ)**.** *Under the setting of Lemma 4.1. Assume we have posterior-mean estimates $\{q_i\}_{i=1}^G$ satisfying the uniform accuracy condition $|q_i - q_i^\star| \le \epsilon$, $\forall i$. We define $\mu_{-j} := \frac{1}{G-1}\sum_{i\neq j} q_i$, let $\hat{\jmath} := \arg\min_{j\in[G]} \left|\mu_{-j} - \rho\right|$, $\hat{p}_{-\hat{\jmath}} := \frac{1}{G-1}\sum_{i\neq\hat{\jmath}} Y_i$, and fix any $\delta \in (0, 1)$. Then, with probability at least $1 - \delta$, we have*

$$\left|\hat{p}_{-\hat{\jmath}} - \rho\right| \le \min_{j\in[G]} \left|\mu_{-j}^\star - \rho\right| + 2\epsilon + \sqrt{\frac{\log(2/\delta)}{2(G-1)}}.$$

The proof can be found in Appendix A.1. It implies that pruning can reduce the posterior-mean deviation to a target ratio ρ, and if the posterior estimates q_i are accurate, then posterior-guided pruning is $O(\epsilon)$-close to the true-posterior pruning in terms of deviation from ρ. Therefore, setting $\rho = 0.5$ can enhance the learning signals and improve the effectiveness of training.

4.2 Quality Prediction Head

We have shown that if we have an accurate posterior estimate q_i for each rollout, we can prune rollouts to control the within-group positive ratio and improve the learning signal. However, q_i is not directly observable during generation, especially when we want to prune a rollout early. To operationalize Sec. 4.1, we first construct an early-stage *quality score* s_i for a partial rollout, and then map this score to a posterior estimate $q_i \in [0, 1]$.

Quality Score Prediction. Previous studies (Kang et al., 2025; Fu et al., 2025) introduce internal uncertainty signals, trace confidence, based on the log-probability of next tokens, which can serve as *quality scores* s_i. However, these metrics are only indirect proxies of rollout quality. Since they are computed from token-level likelihood without task supervision, they are not guaranteed to align with the final success label. As shown in Fig. 2(a), a failure example indicates that reflection-related tokens tend to receive low confidence despite being beneficial, whereas formula-heavy tokens can receive high confidence even under incorrect reasoning. Therefore, we turn to the model's hidden representations to generate quality scores of rollouts. Like the next token prediction head in language models, we can also add a *rollout quality head* to the backbone model, which can be a simple 2-layer MLP. Since RL naturally provides labeled rollouts, we can train the quality head on-the-fly using cross-entropy loss, whose gradient will be detached from backbone model to avoid possible overhead. To evaluate the effectiveness of the scores from quality head, we collect 4,000 rollouts from two datasets. As shown in Fig. 2(b), the scores given by quality head as quality scores can distinguish the correct rollouts

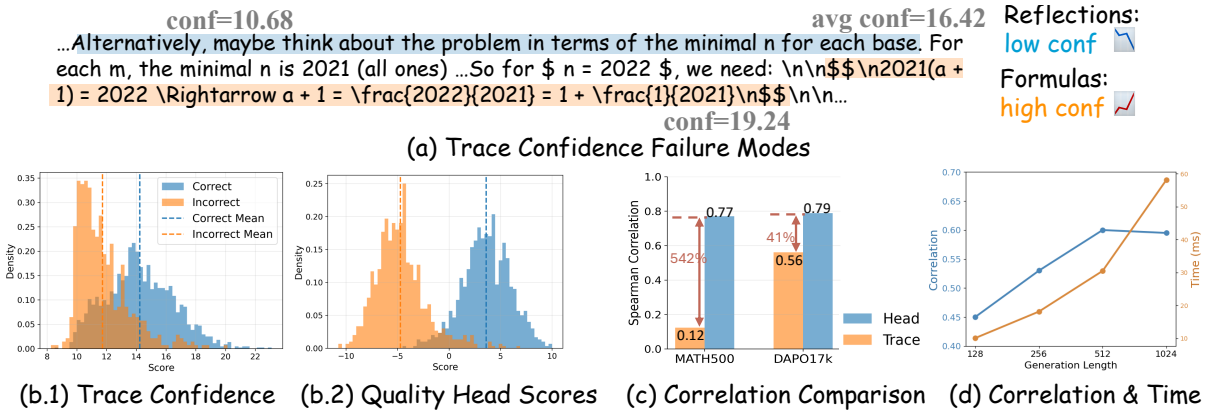

Figure 2: (a) Trace Confidence Failure Modes: Reflection-related tokens tend to receive low confidence despite being beneficial, whereas formula-heavy tokens can receive high confidence even under incorrect reasoning. (b) Distribution Comparison. Trace confidence in (b.1) is less separable between correct/incorrect than quality head scores in (b.2). (c) Correlation Comparison. Quality-head scores achieve consistently higher correlation, measured by Spearman rank correlation between the predicted scores (quality scores or trace confidence) and the binary correctness of final answers on the Math500 and Dapo17k datasets. (d) Generation Length v.s. Correlation & Time Cost. The time cost increases as the generation length increases, while the correlation plateaus when the length reaches 512. All the data is generated by Qwen3-4B model on 400 prompts from Dapo17k and Math500 dataset with 10 rollouts per sample.

from incorrect ones, with separable distributions of the two categories. Also, quality head scores show a stable Spearman rank correlation across datasets (Fig. 2(c)).

In our experiments, the quality head is implemented as a 2-layer MLP with hidden dimension 128. Its overhead is negligible compared to the backbone: for a sequence with batch size 1 and length 2048 on Qwen3-8B, it adds only 2.15 GFLOPs, which is about 0.007% of the backbone's 30.92 TFLOPs.

Detection Length. Training-time pruning requires choosing an intermediate length to evaluate the quality score. Fig. 2(d) reports the correlation between intermediate quality head scores and final correctness, as well as the generation time to reach each length. We find that early detection is reliable, and choose $L_{\text{detect}} = 512$ to balance pruning reliability and time cost.

Probability Calibration. Given the quality-head score s_i, we need a probability-like posterior estimate $q_i \in [0, 1]$ to instantiate Sec. 4.1. Since the raw score scale may shift during training, we adopt an *online binned probability estimator* to map scores to posteriors (Zadrozny and Elkan, 2001). Concretely, we first normalize the score to $s'_i \in [0, 1]$ and assign it to one of B uniform bins denoted as $b(s')$. For each bin, we maintain the numbers of historical positive and negative rollouts (with a sliding buffer), and estimate the posterior success probability by:

$$q(s') = P(Y = 1|b(s')) = \frac{\pi P(b(s')|Y = 1)}{\pi P(b(s')|Y = 1) + (1 - \pi)P(b(s')|Y = 0)},$$

where $\pi = P(Y = 1)$, $P(b(s')|Y = 0)$ and $P(b(s')|Y = 1)$ are estimated by historical information from previous steps maintaining with a sliding buffer.

With $q_i = P(y = 1|s_i)$ as an estimate of the rollout success probability, we assign each rollout a *survival probability* p_i. The design goal is twofold: (i) the expected keep ratio matches a target κ, and (ii) the kept rollouts have a controlled positive ratio close to ρ. We achieve this by defining p_i as a monotonic function of $(\rho - q_i)$ and normalizing it to satisfy the keep-rate constraint. Sampling rollouts according to $\{p_i\}$ allows us to prune multiple rollouts in one step while steering the within-group balance toward ρ. More details can be found in Appendix A.4.

4.3 System Design

To enable efficient RL training, we adopt the commonly used framework verl (Sheng et al., 2024) of frontend-backend architecture and implement rollout pruning inside the generation backend, vLLM (Kwon et al., 2023). An overview is given

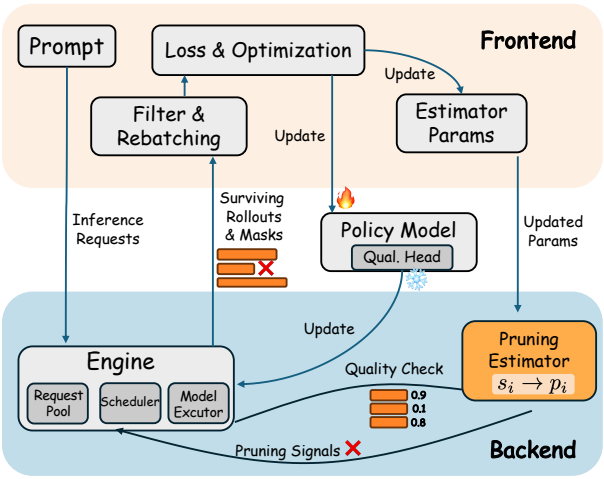

Figure 3: Illustration of System Design.

in Fig. 3. In each training step, we (i) generate rollouts, (ii) compute log-probabilities/advantages, and (iii) update the policy. The frontend orchestrates data and runs log-probability computation and policy updates, while the backend provides high-throughput rollout generation. **(i) Backend.** The frontend sends rollout-generation requests to the backend. The backend maintains a request pool and dynamically batches active sequences for GPU execution. When a rollout first reaches the detection length L_{detect}, the backend evaluates its quality and samples a pruning decision according to the survival probability (Sec. 4.2).

Pruned rollouts are immediately removed from the request pool, so the scheduler can reallocate the freed capacity to other active sequences, reducing the overall generation time without lowering GPU utilization. **(ii) Frontend.** The backend returns the pruning masks together with the generated rollouts. The frontend filters out pruned rollouts and re-batches the surviving ones to compute log-probabilities and advantages, followed by policy optimization. This reduces the log-probability computation and backpropagation cost roughly in proportion to the number of surviving rollouts. **(iii) Quality head.** Each rollout is naturally labeled by its final reward, so we can collect training data for the quality head on the fly. We update the quality head with a cross-entropy loss, while stopping gradients to the backbone model. As a result, the additional overhead is negligible. For more details, please refer to Fig. 3 and Appendix A.5.

4.4 Test-time Scaling.

At test time, the trained quality head can also naturally serve as a correctness predictor. Given a set of completed reasoning traces, we apply the head to obtain a score s_i for each candidate. Instead of a naive majority vote, we use these scores to calculate voting weights. Since s_i is an uncalibrated logit-like score, we convert scores to rank-based weights by sorting candidates and linearly rescaling their ranks to $[0, 1]$.

5 Experiment

5.1 Experimental Settings

We build system based on verl (Sheng et al., 2024) framework for training and vLLM (Kwon et al., 2023) framework as inference engine. We conduct experiments on LLMs of different sizes and different series: Qwen-3 (1.7B, 4B, 8B), and LLaMA-3.2 (1.7B). We compare vanilla GRPO (Shao et al., 2024) and DAPO (Yu et al., 2025c) with their AR-RoL-equipped variants on Math500 (Hendrycks et al., 2021), OlympiadBench (He et al., 2024), and MinervaMath (Lewkowycz et al., 2022) using average accuracy, and on AMC'23, AIME'24, and AIME'25 using pass@16. When training with our method, we use a cold-start period of 20 steps to initialize the quality head and the pruning estimator. For test-time scaling, we report maj@32 and compare our method against vanilla GRPO and trace score from DeepConf (Fu et al., 2025). Models are trained on the Dapo-Math-17K (Yu et al., 2025c) dataset with a maximum sequence length of 8,192. The learning rate is set to 1×10^{-6}, and the group size is set to 16. Other hyperparameters include $\kappa = 0.5$, $\rho = 0.5$, $L_{\text{detect}} = 512$. For GRPO algorithm, we set $\epsilon_{low} = \epsilon_{high} = 0.2$, and for DAPO algorithm, we change ϵ_{high} to 0.28. The experiments are conducted on NVIDIA GH200 GPUs.

5.2 Details of the Datasets

Dapo-Math-17k. DAPO-Math-17k (Yu et al., 2025c) is a curated collection of mathematical problems paired with verifiable final answers. The problems are sourced from online math resources and manual annotations, and are transformed to require an integer final answer to facilitate easy parsing. The dataset is commonly used for RLVR-style training and evaluation on math reasoning tasks.

Math500. Math500 (Lightman et al., 2023) is a subset of the MATH (Hendrycks et al., 2021) dataset, containing 500 high-school-level problems. It covers a wide range of topics, including algebra, geometry, and precalculus, and is commonly

Table 1: Performance Comparison on GRPO. We compare our method with vanilla GRPO on six benchmarks across four models, and also report speedup.

Method	Math500	Minervamath	OlympiadBench	AMC'23	AIME'24	AIME'25	Avg	Speedup
				Qwen-3-1.7B-Base				
GRPO	60.89	**17.65**	18.55	75.00	20.00	**16.67**	34.79	-
+ARROL	**62.30**	16.91	**20.81**	**82.50**	**23.33**	**16.67**	**37.09**	1.61×
				Qwen-3-4B-Base				
GRPO	79.64	**30.88**	31.37	87.50	36.67	40.00	51.01	-
+ARROL	**80.04**	28.67	**33.33**	**92.50**	**40.00**	**46.67**	**53.54**	1.63×
				Qwen-3-8B-Base				
GRPO	81.25	32.36	**34.69**	**95.00**	56.67	**40.00**	56.66	-
+ARROL	**81.45**	**34.19**	33.18	**95.00**	**66.67**	**46.67**	**59.53**	1.62×
				LLama-3.2-1B-Instruct				
GRPO	24.20	3.31	2.26	45.00	13.33	0.00	14.63	-
+ARROL	**29.03**	**4.04**	**4.37**	**47.50**	**16.67**	**3.33**	**17.49**	1.67×

Table 2: Performance Comparison on DAPO. We compare our method with vanilla DAPO on six benchmarks on Qwen-3-1.7B-Base, and also report speedup.

Method	Math500	Minervamath	OlympiadBench	AMC'23	AIME'24	AIME'25	Avg	Speedup
				Qwen-3-1.7B-Base				
DAPO	**62.10**	**20.96**	20.51	**75.00**	20.00	20.00	36.43	-
+ARROL	**62.10**	**20.96**	**20.97**	72.50	**33.33**	**26.67**	**39.42**	1.70×

used for comprehensive evaluation of mathematical reasoning.

Minervamath. Minervamath (Lewkowycz et al., 2022) consists of 272 problems, sourced primarily from MIT OpenCourseWare courses. It is designed to evaluate the mathematical and quantitative reasoning capabilities of LLMs.

OlympiadBench. OlympiadBench (He et al., 2024) contains 8,476 Olympiad-level math and physics problems, including problems from the Chinese college entrance exam. Each problem is accompanied by expert annotations with step-by-step reasoning.

AMC'23. AMC'23 is a dataset of 40 problems from the 2023 American Mathematics Competitions (AMC). The final answer is an integer ranging from 0 to 999.

AIME'24/AIME'25. Each dataset contains 30 challenging problems from the American Invitational Mathematics Examination (AIME). These questions require deep knowledge and techniques, especially in combinatorics and geometry. The final answer is an integer ranging from 0 to 999.

For small datasets such as AMC/AIME, repeated sampling is often used to reduce evaluation variance. Results are typically reported as avg@k, i.e., the average accuracy over k independent repeats, or pass@k, i.e., whether at least one of the k samples is correct. Maj@k is also commonly used, defined as the accuracy of the majority-vote answer among k repeats.

5.3 Main Results

Performances on GRPO. We report performance comparisons between vanilla GRPO and GRPO equipped with ARROL, as shown in Table 1. Across most benchmarks, ARROL consistently outperforms vanilla GRPO, improving average accuracy by $+2.30$ to $+2.87$ on the Qwen-3 series and by $+2.86$ on LLaMA-3.2. Notably, the gains are larger on harder benchmarks: for example, ARROL improves AMC'23 by $+7.50$ on Qwen-3-

Table 3: Performance Comparison of Test-time Voting. We compare our method with GRPO and Deepconf method on three benchmarks across three models.

Method	AMC'23	AIME'24	AIME'25
Qwen-3-1.7B-Base			
Majority	55.0	16.7	3.3
Deepconf	57.5	16.7	6.7
ARRoL	**60.0**	**23.3**	**13.3**
Qwen-3-4B-Base			
Majority	72.5	26.7	20.0
Deepconf	72.5	33.3	23.3
ARRoL	**82.5**	**36.7**	**26.7**
Qwen-3-8B-Base			
Majority	75.0	23.3	26.7
Deepconf	80.0	23.3	23.3
ARRoL	**85.0**	**33.3**	**33.3**
LLama-3.2-1B-instruct			
Majority	10.0	0.0	**0.0**
Deepconf	15.0	3.3	**0.0**
ARRoL	**17.5**	**10.0**	**0.0**

1.7B and improves AIME'24 by $+10.00$ on Qwen-3-8B (and $+6.67$ on AIME'25). Meanwhile, we observe small regressions on a few datasets (e.g., Minervamath on Qwen-3-1.7B/4B), but the overall improvement remains consistent. In addition to better performance, ARRoL substantially reduces training cost, achieving a stable $1.6-1.7\times$ end-to-end speedup across model sizes. These results support a "less is more" effect: pruning yields fewer but more balanced samples, leading to both higher accuracy and better efficiency, and the gains are robust across model families and sizes. Finally, the quality head reaches $\sim$80% prediction accuracy (e.g., 82.37% on Qwen3-1.7B), indicating it can be reliably trained within our pipeline for early-stage pruning decisions.

Performances on DAPO. We further evaluate ARRoL on DAPO by comparing vanilla DAPO with its ARRoL-equipped variant. The results are reported in Table 2. Overall, ARRoL achieves the best performance on most benchmarks, improving average accuracy by $+2.99$ while maintaining a $1.70\times$ end-to-end speedup. These results suggest that ARRoL generalizes well across RLVR algorithms and delivers consistent efficiency gains.

Test-time Scaling. To evaluate the quality head at inference time, we compare ARRoL against vanilla majority voting and DeepConf (Fu et al., 2025), which uses log-likelihood-based trace confidence as voting weights for final-answer aggregation. As shown in Table 3, while DeepConf improves over majority vote, the learned quality head provides consistent gains across datasets and models, yielding up to $+8.33$ additional improvement over DeepConf. These results suggest that the quality head trained during RLVR can serve as reliable confidence weights for test-time voting, outperforming model-intrinsic heuristic signals (e.g., DeepConf) that are not guaranteed to align with final-answer correctness.

5.4 Ablation Studies

Table 4: Performance Comparison against Random Pruning. $\hat{\rho}$ is the fraction of positive (reward=1) rollouts during training. For binary rewards, $\hat{\rho}(1-\hat{\rho})$ is proportional to the within-group reward variance and is maximized at $\hat{\rho}=0.5$.

Method	AMC23	AIME24	AIME25	$\mathbb{E}[\hat{\rho}]$	$\mathbb{E}[\hat{\rho}(1-\hat{\rho})]$
Qwen-3-4B-Base					
Random	79.34	26.47	31.98	0.32	0.21
ARRoL	80.04	28.67	33.33	0.40	0.23
LLama-3.2-1B-instruct					
Random	22.18	2.94	3.02	0.14	0.11
ARRoL	29.03	4.04	4.37	0.23	0.14

Table 5: Efficiency decomposition for Qwen-3-1.7B-Base across training phases: rollout generation, log-probability computation, and model update.

Time/s	Generation	Logprob	Update
GRPO	106.82	18.40	63.05
ARRoL	72.96 (1.46×)	10.02 (1.84×)	30.26 (2.08×)

Comparison with Random Pruning. To validate the effectiveness of ARRoL, we compare it with random pruning in Table 4. ARRoL

Table 6: Average accuracy on Math500, MinervaMath, and OlympiadBench, and training speedup under different rollout keep ratios κ for Qwen-3-1.7B-Base.

κ	0.25	0.5	0.75	1
Avg Acc	32.46	33.34	32.68	32.36
Speedup	2.33×	1.61×	1.17×	1.00×

consistently outperforms random pruning across datasets. We further report the within-group positive ratio during training. Specifically, for each prompt group we compute $\hat{\rho}$ as the fraction of positive (reward=1) rollouts during training, and report $\mathbb{E}[\hat{\rho}]$ and $\mathbb{E}[\hat{\rho}(1-\hat{\rho})]$ (average across groups). For binary rewards, $\hat{\rho}(1-\hat{\rho})$ is proportional to the within-group reward variance and is maximized at $\hat{\rho} = 0.5$ (Bae et al., 2025), indicating stronger non-degenerate learning signals for group-normalized updates. As shown in Table 4, ARROL drives groups closer to balanced outcomes 0.5 and increases $\mathbb{E}[\hat{\rho}(1-\hat{\rho})]$, which is consistent with stronger learning signals and better final performance.

Efficiency Decomposition. We further analyze the source of the efficiency gains by decomposing training time into different phases, as shown in Table 5. Overall, our method accelerates all phases. For log-probability computation and model updates, the time is reduced by about $2\times$, since pruning discards roughly half of the rollouts. In contrast, the speedup for rollout generation is smaller ($1.46\times$), because we first generate all sequences up to a threshold length L_{detect} before pruning half of the rollouts.

Wall-clock convergence. We evaluate wall-clock convergence by plotting training reward against wall-clock time, as shown in Fig. 4. Compared with GRPO, our pruning based training reaches the same reward level in less time and attains higher reward earlier across most of training, indicating improved time-to-reward and faster wall-clock convergence.

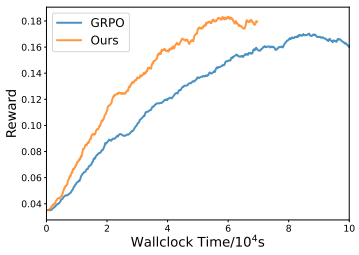

Figure 4: Wall-clock convergence of Qwen-3-1.7B-Base training.

Ablation Study on keep ratio κ. In our main experiments, we set the keep ratio κ to 0.5. To study how κ affects both effectiveness and efficiency, we evaluate several values of κ. As shown in Table 6, a smaller κ yields larger speedup since fewer rollouts are kept during pruning. Performance generally improves as κ decreases, suggesting that pruning can also help by selecting more balanced sample subset. However, when $\kappa = 0.25$, too many rollouts are removed, leading to a slight performance drop. Overall, $\kappa = 0.5$ provides a good trade-off between accuracy and efficiency.

6 Conclusion

We presented ARROL, an online rollout pruning approach for RLVR that prunes rollouts *during* generation while explicitly steering the surviving group toward a more balanced 0/1 reward composition, strengthening learning signals. ARROL trains a lightweight quality head on-the-fly to predict the success probability of partial rollouts, and uses them to make early pruning decisions under a target keep ratio. To realize efficiency gains, we further implemented a system design. Empirically, on different models, ARROL consistently improves accuracy while achieving up to $1.7\times$ training speedup. Moreover, the learned quality head can also be used at test time as voting weights, yielding additional gains over naive majority voting. Overall, ARROL demonstrates a practical "less rollouts, more learning" paradigm for efficient and effective RLVR training and test-time scaling.

Limitations

Our study mainly focuses on mathematical RLVR tasks with verifiable rewards; while the core idea (online pruning guided by a correctness predictor and balance control) is general and could be extended to other reward-based RL scenarios, such as UI interaction or tool-use agents, we do not validate these domains in this work. In addition, training-time pruning needs to generate tokens up to an intermediate detection length to evaluate partial rollouts (we set $L_{\text{detect}} = 512$), so the rollout-generation speedup can be smaller than the savings in later phases because sequences must reach this threshold before pruning takes effect.

Acknowledgement

This work is supported by NSF (2134079). The content of the information in this document does not necessarily reflect the position or the policy of the Government, and no official endorsement should be inferred. The U.S. Government is authorized to reproduce and distribute reprints for Government purposes notwithstanding any copyright notation here on.

References

Ehsan Aghazadeh, Ahmad Ghasemi, Hedyeh Beyhaghi, and Hossein Pishro-Nik. 2025. Cges: Confidence-guided early stopping for efficient and accurate self-consistency. *arXiv preprint arXiv:2511.02603*.

Mengting Ai, Tianxin Wei, Yifan Chen, Zhichen Zeng, Ritchie Zhao, Girish Varatkar, Bita Darvish Rouhani, Xianfeng Tang, Hanghang Tong, and Jingrui He. 2025. Resmoe: Space-efficient compression of mixture of experts llms via residual restoration. In *Proceedings of the 31st ACM SIGKDD Conference on Knowledge Discovery and Data Mining V. 1*, pages 1–12.

Sanghwan Bae, Jiwoo Hong, Min Young Lee, Hanbyul Kim, JeongYeon Nam, and Donghyun Kwak. 2025. Online difficulty filtering for reasoning oriented reinforcement learning. *arXiv preprint arXiv:2504.03380*.

Yikun Ban, Yuchen Yan, Arindam Banerjee, and Jingrui He. 2023. Neural exploitation and exploration of contextual bandits. *arXiv preprint arXiv:2305.03784*.

Wenxuan Bao, Ruxi Deng, Ruizhong Qiu, Tianxin Wei, Hanghang Tong, and Jingrui He. 2025. Latte: Collaborative test-time adaptation of vision-language models in federated learning. In *Proceedings of the IEEE/CVF International Conference on Computer Vision*.

Burak Bartan, Ruizhong Qiu, Rafael Esteves, Yuwei Ren, Weiliang Will Zeng, and An Chen. 2025. FineAMP: optimization-based automatic mixed precision quantization for efficient diffusion model inference. *The 17th International OPT Workshop on Optimization for Machine Learning*.

Yuanchen Bei, Tianxin Wei, Xuying Ning, Yanjun Zhao, Zhining Liu, Xiao Lin, Yada Zhu, Hendrik Hamann, Jingrui He, and Hanghang Tong. 2026. Mem-gallery: Benchmarking multimodal long-term conversational memory for mllm agents. *arXiv preprint arXiv:2601.03515*.

Sirui Chen, Yunzhe Qi, Mengting Ai, Yifan Sun, Ruizhong Qiu, Jiaru Zou, and Jingrui He. 2026a. Influence-preserving proxies for gradient-based data selection in LLM finetuning. In *The Fourteenth International Conference on Learning Representations*.

Sirui Chen, Yunzhe Qi, Mengting Ai, Yifan Sun, Ruizhong Qiu, Jiaru Zou, and Jingrui He. 2026b. Influence-preserving proxies for gradient-based data selection in llm finetuning. In *The Fourteenth International Conference on Learning Representations*.

Chengming Cui, Tianxin Wei, Ziyi Chen, Ruizhong Qiu, Zhichen Zeng, Zhining Liu, Xuying Ning, Duo Zhou, and Jingrui He. 2026. AdaFuse: adaptive ensemble decoding with test-time scaling for LLMs. *arXiv preprint*.

Muzhi Dai, Chenxu Yang, and Qingyi Si. 2025. S-grpo: Early exit via reinforcement learning in reasoning models. *arXiv preprint arXiv:2505.07686*.

Tim Dettmers, Artidoro Pagnoni, Ari Holtzman, and Luke Zettlemoyer. 2023. Qlora: Efficient finetuning of quantized llms. *Advances in neural information processing systems*, 36:10088–10115.

Ning Ding, Yujia Qin, Guang Yang, Fuchao Wei, Zonghan Yang, Yusheng Su, Shengding Hu, Yulin Chen, Chi-Min Chan, Weize Chen, and 1 others. 2023. Parameter-efficient fine-tuning of large-scale pre-trained language models. *Nature machine intelligence*, 5(3):220–235.

Alex ZH Dou, Zhongwei Wan, Dongfei Cui, Xin Wang, Jing Xiong, Haokun Lin, Chaofan Tao, Shen Yan, and Mi Zhang. 2025. Enhancing test-time scaling of large language models with hierarchical retrieval-augmented mcts. *arXiv preprint arXiv:2507.05557*.

Elias Frantar, Saleh Ashkboos, Torsten Hoefler, and Dan Alistarh. 2022. Gptq: Accurate post-training quantization for generative pre-trained transformers. *arXiv preprint arXiv:2210.17323*.

Yichao Fu, Xuewei Wang, Yuandong Tian, and Jiawei Zhao. 2025. Deep think with confidence. *arXiv preprint arXiv:2508.15260*.

Jianping Gou, Baosheng Yu, Stephen J Maybank, and Dacheng Tao. 2021. Knowledge distillation: A survey. *International journal of computer vision*, 129(6):1789–1819.

Daya Guo, Dejian Yang, Haowei Zhang, Junxiao Song, Ruoyu Zhang, Runxin Xu, Qihao Zhu, Shirong Ma, Peiyi Wang, Xiao Bi, and 1 others. 2025. Deepseek-r1: Incentivizing reasoning capability in llms via reinforcement learning. *arXiv preprint arXiv:2501.12948*.

Chaoqun He, Renjie Luo, Yuzhuo Bai, Shengding Hu, Zhen Thai, Junhao Shen, Jinyi Hu, Xu Han, Yujie Huang, Yuxiang Zhang, and 1 others. 2024. Olympiadbench: A challenging benchmark for promoting agi with olympiad-level bilingual multimodal scientific problems. In *Proceedings of the 62nd Annual Meeting of the Association for Computational Linguistics (Volume 1: Long Papers)*, pages 3828–3850.

Jingkai He, Tianjian Li, Erhu Feng, Dong Du, Qian Liu, Tao Liu, Yubin Xia, and Haibo Chen. 2025. History rhymes: Accelerating llm reinforcement learning with rhymerl. *arXiv preprint arXiv:2508.18588*.

Xinyu He, Chenhan Xiao, Haoran Li, Ruizhong Qiu, Zhe Xu, Yang Weng, Jingrui He, and Hanghang Tong. 2026. PowerGrow: feasible co-growth of structures and dynamics for power grid synthesis. In *Proceedings of the 32nd ACM SIGKDD Conference on Knowledge Discovery and Data Mining*.

Dan Hendrycks, Collin Burns, Saurav Kadavath, Akul Arora, Steven Basart, Eric Tang, Dawn Song, and Jacob Steinhardt. 2021. Measuring mathematical problem solving with the math dataset. *arXiv preprint arXiv:2103.03874*.

Wassily Hoeffding. 1963. Probability inequalities for sums of bounded random variables. *Journal of the American statistical association*, 58(301):13–30.

Edward J Hu, Yelong Shen, Phillip Wallis, Zeyuan Allen-Zhu, Yuanzhi Li, Shean Wang, Liang Wang, Weizhu Chen, and 1 others. 2022. Lora: Low-rank adaptation of large language models. *Iclr*, 1(2):3.

Wei Huang, Yi Ge, Shuai Yang, Yicheng Xiao, Huizi Mao, Yujun Lin, Hanrong Ye, Sifei Liu, Ka Chun Cheung, Hongxu Yin, and 1 others. 2025. Qerl: Beyond efficiency–quantization-enhanced reinforcement learning for llms. *arXiv preprint arXiv:2510.11696*.

Aaron Jaech, Adam Kalai, Adam Lerer, Adam Richardson, Ahmed El-Kishky, Aiden Low, Alec Helyar, Aleksander Madry, Alex Beutel, Alex Carney, and 1 others. 2024. Openai o1 system card. *arXiv preprint arXiv:2412.16720*.

Zhewei Kang, Xuandong Zhao, and Dawn Song. 2025. Scalable best-of-n selection for large language models via self-certainty. *arXiv preprint arXiv:2502.18581*.

Woosuk Kwon, Zhuohan Li, Siyuan Zhuang, Ying Sheng, Lianmin Zheng, Cody Hao Yu, Joseph Gonzalez, Hao Zhang, and Ion Stoica. 2023. Efficient memory management for large language model serving with pagedattention. In *Proceedings of the 29th symposium on operating systems principles*, pages 611–626.

Nathan Lambert, Jacob Morrison, Valentina Pyatkin, Shengyi Huang, Hamish Ivison, Faeze Brahman, Lester James V Miranda, Alisa Liu, Nouha Dziri, Shane Lyu, and 1 others. 2024. Tulu 3: Pushing frontiers in open language model post-training. *arXiv preprint arXiv:2411.15124*.

Aitor Lewkowycz, Anders Andreassen, David Dohan, Ethan Dyer, Henryk Michalewski, Vinay Ramasesh, Ambrose Slone, Cem Anil, Imanol Schlag, Theo Gutman-Solo, and 1 others. 2022. Solving quantitative reasoning problems with language models. *Advances in neural information processing systems*, 35:3843–3857.

Gaotang Li, Ruizhong Qiu, Xiusi Chen, Heng Ji, and Hanghang Tong. 2025. Beyond log likelihood: Probability-based objectives for supervised fine-tuning across the model capability continuum. *arXiv preprint*.

Hunter Lightman, Vineet Kosaraju, Yuri Burda, Harrison Edwards, Bowen Baker, Teddy Lee, Jan Leike, John Schulman, Ilya Sutskever, and Karl Cobbe. 2023. Let's verify step by step. In *The Twelfth International Conference on Learning Representations*.

Haokun Lin, Haoli Bai, Zhili Liu, Lu Hou, Muyi Sun, Linqi Song, Ying Wei, and Zhenan Sun. 2024a. Mope-clip: Structured pruning for efficient vision-language models with module-wise pruning error metric. In *Proceedings of the IEEE/CVF conference on computer vision and pattern recognition*, pages 27370–27380.

Haokun Lin, Xinle Jia, Shaozhen Liu, Shujun Xia, Weitao Huang, Haobo Xu, Junyang Li, Yicheng Xiao, Xingrun Xing, Ziyu Guo, and 1 others. 2026. Efficient diffusion language models: A comprehensive survey. *Authorea Preprints*.

Haokun Lin, Haobo Xu, Yichen Wu, Jingzhi Cui, Yingtao Zhang, Linzhan Mou, Linqi Song, Zhenan Sun, and Ying Wei. 2024b. Duquant: Distributing outliers via dual transformation makes stronger quantized llms. *Advances in Neural Information Processing Systems*, 37:87766–87800.

Haokun Lin, Haobo Xu, Yichen Wu, Ziyu Guo, Renrui Zhang, Zhichao Lu, Ying Wei, Qingfu Zhang, and Zhenan Sun. 2025a. Quantization meets dllms: A systematic study of post-training quantization for diffusion llms. *arXiv preprint arXiv:2508.14896*.

Zhihang Lin, Mingbao Lin, Yuan Xie, and Rongrong Ji. 2025b. Cppo: Accelerating the training of group relative policy optimization-based reasoning models. *arXiv preprint arXiv:2503.22342*.

Bingshuai Liu, Ante Wang, Zijun Min, Liang Yao, Haibo Zhang, Yang Liu, Anxiang Zeng, and Jinsong Su. 2025a. Spec-rl: Accelerating on-policy reinforcement learning via speculative rollouts. *arXiv preprint arXiv:2509.23232*.

Lihui Liu, Zihao Wang, Ruizhong Qiu, Yikun Ban, Eunice Chan, Yangqiu Song, Jingrui He, and Hanghang Tong. 2024. Logic query of thoughts: Guiding large language models to answer complex logic queries with knowledge graphs. *arXiv preprint*.

Lihui Liu, Zihao Wang, Dawei Zhou, Ruijie Wang, Yuchen Yan, Bo Xiong, Sihong He, and Hanghang Tong. 2025b. Few-shot knowledge graph completion via transfer knowledge from similar tasks. In *Proceedings of the 34th ACM International Conference on Information and Knowledge Management*, pages 4960–4965.

Lihui Liu and Yuchen Yan. 2026. Morgan: To bridge mixture of experts and spectral graph neural network. In *Proceedings of the AAAI Conference on Artificial Intelligence*, volume 40, pages 23783–23791.

Zichen Liu, Changyu Chen, Wenjun Li, Penghui Qi, Tianyu Pang, Chao Du, Wee Sun Lee, and Min Lin. 2025c. Understanding r1-zero-like training: A critical perspective. *arXiv preprint arXiv:2503.20783*.

Niklas Muennighoff, Zitong Yang, Weijia Shi, Xiang Lisa Li, Li Fei-Fei, Hannaneh Hajishirzi, Luke Zettlemoyer, Percy Liang, Emmanuel Candès, and Tatsunori B Hashimoto. 2025. s1: Simple test-time

scaling. In *Proceedings of the 2025 Conference on Empirical Methods in Natural Language Processing*, pages 20286–20332.

Ruizhong Qiu, Jun-Gi Jang, Xiao Lin, Lihui Liu, and Hanghang Tong. 2024a. TUCKET: a tensor time series data structure for efficient and accurate factor analysis over time ranges. In *Proceedings of the VLDB Endowment 17*, 13.

Ruizhong Qiu, Gaotang Li, Ting-Wei Li, Tianxin Wei, Jingrui He, and Hanghang Tong. 2025a. Efficient inference scaling for safety assurance. *NeurIPS 2025 Workshop on Vision–Language Model Real-World Deployment*.

Ruizhong Qiu, Ting-Wei Li, Gaotang Li, and Hanghang Tong. 2026a. Graph homophily booster: Reimagining the role of discrete features in heterophilic graph learning. In *The Fourteenth International Conference on Learning Representations*.

Ruizhong Qiu, Zhiqing Sun, and Yiming Yang. 2022. DIMES: a differentiable meta solver for combinatorial optimization problems. In *Advances in Neural Information Processing Systems 35*.

Ruizhong Qiu, Dingsu Wang, Lei Ying, H. Vincent Poor, Yifang Zhang, and Hanghang Tong. 2023. Reconstructing graph diffusion history from a single snapshot. In *Proceedings of the 29th ACM SIGKDD Conference on Knowledge Discovery and Data Mining*.

Ruizhong Qiu, Zhe Xu, Wenxuan Bao, and Hanghang Tong. 2025b. Ask, and it shall be given: On the Turing completeness of prompting. In *The Thirteenth International Conference on Learning Representations*.

Ruizhong Qiu, Hanqing Zeng, Yinglong Xia, Yiwen Meng, Ren Chen, Jiarui Feng, Dongqi Fu, Qifan Wang, Jiayi Liu, Jun Xiao, Xiangjun Fan, Benyu Zhang, Hong Li, Zhining Liu, Hyunsik Yoo, Zhichen Zeng, Tianxin Wei, and Hanghang Tong. 2026b. ReMix: reinforcement routing for mixtures of LoRAs in LLM finetuning. *Under review*.

Ruizhong Qiu, Weiliang Will Zeng, James Ezick, Christopher Lott, and Hanghang Tong. 2024b. How efficient is llm-generated code? a rigorous & high-standard benchmark. *arXiv preprint arXiv:2406.06647*.

Zhihong Shao, Peiyi Wang, Qihao Zhu, Runxin Xu, Junxiao Song, Xiao Bi, Haowei Zhang, Mingchuan Zhang, YK Li, Yang Wu, and 1 others. 2024. Deepseekmath: Pushing the limits of mathematical reasoning in open language models. *arXiv preprint arXiv:2402.03300*.

Guangming Sheng, Chi Zhang, Zilingfeng Ye, Xibin Wu, Wang Zhang, Ru Zhang, Yanghua Peng, Haibin Lin, and Chuan Wu. 2024. verl: Volcano engine reinforcement learning for llm.

Charlie Snell, Jaehoon Lee, Kelvin Xu, and Aviral Kumar. 2024. Scaling llm test-time compute optimally can be more effective than scaling model parameters. *arXiv preprint arXiv:2408.03314*.

Ashish Vaswani, Noam Shazeer, Niki Parmar, Jakob Uszkoreit, Llion Jones, Aidan N Gomez, Łukasz Kaiser, and Illia Polosukhin. 2017. Attention is all you need. *Advances in neural information processing systems*, 30.

Zhongwei Wan, Xin Wang, Che Liu, Samiul Alam, Yu Zheng, Jiachen Liu, Zhongnan Qu, Shen Yan, Yi Zhu, Quanlu Zhang, and 1 others. 2023. Efficient large language models: A survey. *arXiv preprint arXiv:2312.03863*.

Xuezhi Wang, Jason Wei, Dale Schuurmans, Quoc Le, Ed Chi, Sharan Narang, Aakanksha Chowdhery, and Denny Zhou. 2022. Self-consistency improves chain of thought reasoning in language models. *arXiv preprint arXiv:2203.11171*.

Yue Wang, Qiuzhi Liu, Jiahao Xu, Tian Liang, Xingyu Chen, Zhiwei He, Linfeng Song, Dian Yu, Juntao Li, Zhuosheng Zhang, and 1 others. 2025. Thoughts are all over the place: On the underthinking of o1-like llms. *arXiv preprint arXiv:2501.18585*.

Tianxin Wei, Ting-Wei Li, Zhining Liu, Xuying Ning, Ze Yang, Jiaru Zou, Zhichen Zeng, Ruizhong Qiu, Xiao Lin, Dongqi Fu, Zihao Li, Mengting Ai, Duo Zhou, Wenxuan Bao, Yunzhe Li, Gaotang Li, Cheng Qian, Yu Wang, Xiangru Tang, and 10 others. 2026a. Agentic reasoning for large language models: A survey. *arXiv preprint*.

Tianxin Wei, Xuying Ning, Xuxing Chen, Ruizhong Qiu, Yupeng Hou, Yan Xie, Shuang Yang, Zhigang Hua, and Jingrui He. 2025. CoFiRec: coarse-to-fine tokenization for generative recommendation. *arXiv preprint*.

Tianxin Wei, Ruizhong Qiu, Yifan Chen, Yunzhe Qi, Jiacheng Lin, Wenxuan Bao, Wenju Xu, Sreyashi Nag, Ruirui Li, Hanqing Lu, Zhengyang Wang, Chen Luo, Hui Liu, Suhang Wang, Jingrui He, Qi He, and Xianfeng Tang. 2026b. DiffKGW: stealthy and robust diffusion model watermarking. *Transactions on Machine Learning Research*.

Yichen Wu, Hongming Piao, Long-Kai Huang, Renzhen Wang, Wanhua Li, Hanspeter Pfister, Deyu Meng, Kede Ma, and Ying Wei. 2025. Sd-lora: Scalable decoupled low-rank adaptation for class incremental learning. *arXiv preprint arXiv:2501.13198*.

Shujun Xia, Haokun Lin, Yichen Wu, Yinan Zhou, Zixuan Li, Zhongwei Wan, Xingrun Xing, Yefeng Zheng, Xiang Li, Caifeng Shan, and 1 others. 2025. Medrek: Retrieval-based editing for medical llms with key-aware prompts. *arXiv preprint arXiv:2510.13500*.

Xingrun Xing, Zheng Liu, Shitao Xiao, Boyan Gao, Yiming Liang, Wanpeng Zhang, Haokun Lin, Guoqi

Li, and Jiajun Zhang. 2025. Efficientllm: Scalable pruning-aware pretraining for architecture-agnostic edge language models. *arXiv preprint arXiv:2502.06663*.

Haobo Xu, Yuchen Yan, Dingsu Wang, Zhe Xu, Zhichen Zeng, Tarek F Abdelzaher, Jiawei Han, and Hanghang Tong. 2024a. Slog: An inductive spectral graph neural network beyond polynomial filter. In *Forty-first International Conference on Machine Learning*.

Yixuan Even Xu, Yash Savani, Fei Fang, and J Zico Kolter. 2025. Not all rollouts are useful: Down-sampling rollouts in llm reinforcement learning. *arXiv preprint arXiv:2504.13818*.

Zhe Xu, Ruizhong Qiu, Yuzhong Chen, Huiyuan Chen, Xiran Fan, Menghai Pan, Zhichen Zeng, Mahashweta Das, and Hanghang Tong. 2024b. Discrete-state continuous-time diffusion for graph generation. In *Advances in Neural Information Processing Systems 37*.

Yuchen Yan, Yuzhong Chen, Huiyuan Chen, Xiaoting Li, Zhe Xu, Zhichen Zeng, Lihui Liu, Zhining Liu, and Hanghang Tong. 2024a. Thegcn: Temporal heterophilic graph convolutional network. *arXiv preprint arXiv:2412.16435*.

Yuchen Yan, Yongyi Hu, Qinghai Zhou, Lihui Liu, Zhichen Zeng, Yuzhong Chen, Menghai Pan, Huiyuan Chen, Mahashweta Das, and Hanghang Tong. 2024b. Pacer: Network embedding from positional to structural. In *Proceedings of the ACM Web Conference 2024*, pages 2485–2496.

Yuchen Yan, Yongyi Hu, Qinghai Zhou, Shurang Wu, Dingsu Wang, and Hanghang Tong. 2024c. Topological anonymous walk embedding: A new structural node embedding approach. In *Proceedings of the 33rd ACM International Conference on Information and Knowledge Management*, pages 2796–2806.

Yuchen Yan, Aakash Kolekar, Sahika Genc, Wenju Xu, Edward W Huang, Anirudh Srinivasan, Mukesh Jain, Qi He, and Hanghang Tong. 2025. To answer or not to answer (taona): A robust textual graph understanding and question answering approach. In *Findings of the Association for Computational Linguistics: EMNLP 2025*, pages 6360–6376.

Yuchen Yan, Lihui Liu, Yikun Ban, Baoyu Jing, and Hanghang Tong. 2021a. Dynamic knowledge graph alignment. In *Proceedings of the AAAI conference on artificial intelligence*, volume 35, pages 4564–4572.

Yuchen Yan, Si Zhang, and Hanghang Tong. 2021b. Bright: A bridging algorithm for network alignment. In *Proceedings of the web conference 2021*, pages 3907–3917.

Yuchen Yan, Qinghai Zhou, Jinning Li, Tarek Abdelzaher, and Hanghang Tong. 2022. Dissecting cross-layer dependency inference on multi-layered inter-dependent networks. In *Proceedings of the 31st ACM International Conference on Information & Knowledge Management*, pages 2341–2351.

Lianwei Yang, Haokun Lin, Tianchen Zhao, Yichen Wu, Hongyu Zhu, Ruiqi Xie, Zhenan Sun, Yu Wang, and Qingyi Gu. 2025. Lrq-dit: Log-rotation post-training quantization of diffusion transformers for image and video generation. *arXiv preprint arXiv:2508.03485*.

Feng Yao, Liyuan Liu, Dinghuai Zhang, Chengyu Dong, Jingbo Shang, and Jianfeng Gao. Your efficient rl framework secretly brings you off-policy rl training, august 2025. *URL https://fengyao. notion. site/off-policy-rl*.

Hyunsik Yoo, SeongKu Kang, Ruizhong Qiu, Charlie Xu, Fei Wang, and Hanghang Tong. 2025a. Embracing plasticity: Balancing stability and plasticity in continual recommender systems. In *Proceedings of the 48th International ACM SIGIR Conference on Research and Development in Information Retrieval*.

Hyunsik Yoo, Ruizhong Qiu, Charlie Xu, Fei Wang, and Hanghang Tong. 2025b. Generalizable recommender system during temporal popularity distribution shifts. In *Proceedings of the 31st ACM SIGKDD Conference on Knowledge Discovery and Data Mining*.

Hyunsik Yoo, Zhichen Zeng, Jian Kang, Ruizhong Qiu, David Zhou, Zhining Liu, Fei Wang, Charlie Xu, Eunice Chan, and Hanghang Tong. 2024. Ensuring user-side fairness in dynamic recommender systems. In *Proceedings of the ACM Web Conference 2024*.

Qi Yu, Zhichen Zeng, Yuchen Yan, Zhining Liu, Baoyu Jing, Ruizhong Qiu, Ariful Azad, and Hanghang Tong. 2025a. Planetalign: A comprehensive python library for benchmarking network alignment. *arXiv preprint arXiv:2505.21366*.

Qi Yu, Zhichen Zeng, Yuchen Yan, Lei Ying, R Srikant, and Hanghang Tong. 2025b. Joint optimal transport and embedding for network alignment. In *Proceedings of the ACM on Web Conference 2025*, pages 2064–2075.

Qiying Yu, Zheng Zhang, Ruofei Zhu, Yufeng Yuan, Xiaochen Zuo, Yu Yue, Weinan Dai, Tiantian Fan, Gaohong Liu, Lingjun Liu, and 1 others. 2025c. Dapo: An open-source llm reinforcement learning system at scale. *arXiv preprint arXiv:2503.14476*.

Bianca Zadrozny and Charles Elkan. 2001. Obtaining calibrated probability estimates from decision trees and naive bayesian classifiers. In *Icml*, volume 1.

Zhichen Zeng, Wenxuan Bao, Xiao Lin, Ruizhong Qiu, Tianxin Wei, Xuying Ning, Yuchen Yan, Chen Luo, Monica Xiao Cheng, Jingrui He, and 1 others. 2026. Subspace alignment for vision-language model test-time adaptation. *arXiv preprint arXiv:2601.08139*.

Zhichen Zeng, Boxin Du, Si Zhang, Yinglong Xia, Zhining Liu, and Hanghang Tong. 2024a. Hierarchical multi-marginal optimal transport for network alignment. In *Proceedings of the AAAI Conference on Artificial Intelligence*, volume 38, pages 16660–16668.

Zhichen Zeng, Mengyue Hang, Xiaolong Liu, Xiaoyi Liu, Xiao Lin, Ruizhong Qiu, Tianxin Wei, Zhining Liu, Siyang Yuan, Chaofei Yang, and 1 others. 2025a. Hierarchical lora moe for efficient ctr model scaling. *arXiv preprint arXiv:2510.10432*.

Zhichen Zeng, Xiaolong Liu, Mengyue Hang, Xiaoyi Liu, Qinghai Zhou, Chaofei Yang, Yiqun Liu, Yichen Ruan, Laming Chen, Yuxin Chen, and 1 others. 2025b. Interformer: Effective heterogeneous interaction learning for click-through rate prediction. In *Proceedings of the 34th ACM International Conference on Information and Knowledge Management*, pages 6225–6233.

Zhichen Zeng, Ruizhong Qiu, Wenxuan Bao, Tianxin Wei, Xiao Lin, Yuchen Yan, Tarek F Abdelzaher, Jiawei Han, and Hanghang Tong. 2025c. Pave your own path: Graph gradual domain adaptation on fused gromov-wasserstein geodesics. *arXiv preprint arXiv:2505.12709*.

Zhichen Zeng, Ruizhong Qiu, Zhe Xu, Zhining Liu, Yuchen Yan, Tianxin Wei, Lei Ying, Jingrui He, and Hanghang Tong. 2024b. Graph mixup on approximate gromov–wasserstein geodesics. In *Forty-first International Conference on Machine Learning*.

Zhichen Zeng, Qi Yu, Xiao Lin, Ruizhong Qiu, Xuying Ning, Tianxin Wei, Yuchen Yan, Jingrui He, and Hanghang Tong. 2025d. Harnessing consistency for robust test-time llm ensemble. *arXiv preprint arXiv:2510.13855*.

Zhichen Zeng, Si Zhang, Yinglong Xia, and Hanghang Tong. 2023a. Parrot: Position-aware regularized optimal transport for network alignment. In *Proceedings of the ACM web conference 2023*, pages 372–382.

Zhichen Zeng, Ruike Zhu, Yinglong Xia, Hanqing Zeng, and Hanghang Tong. 2023b. Generative graph dictionary learning. In *International Conference on Machine Learning*, pages 40749–40769. PMLR.

Jingxuan Zhang, Yunta Hsieh, Zhongwei Wang, Haokun Lin, Xin Wang, Ziqi Wang, Yingtie Lei, and Mi Zhang. 2026. Quantvla: Scale-calibrated post-training quantization for vision-language-action models. *arXiv preprint arXiv:2602.20309*.

Yizhou Zhang, Ning Lv, Teng Wang, and Jisheng Dang. 2025a. Fastgrpo: Accelerating policy optimization via concurrency-aware speculative decoding and online draft learning. *arXiv preprint arXiv:2509.21792*.

Zongzheng Zhang, Haobo Xu, Zhuo Yang, Chenghao Yue, Zehao Lin, Huan-ang Gao, Ziwei Wang, and Hao Zhao. 2025b. Ta-vla: Elucidating the design space of torque-aware vision-language-action models. *arXiv preprint arXiv:2509.07962*.

Haizhong Zheng, Yang Zhou, Brian R Bartoldson, Bhavya Kailkhura, Fan Lai, Jiawei Zhao, and Beidi Chen. 2025. Act only when it pays: Efficient reinforcement learning for llm reasoning via selective rollouts. *arXiv preprint arXiv:2506.02177*.

Lianmin Zheng, Liangsheng Yin, Zhiqiang Xie, Chuyue Livia Sun, Jeff Huang, Cody Hao Yu, Shiyi Cao, Christos Kozyrakis, Ion Stoica, Joseph E Gonzalez, and 1 others. 2024. Sglang: Efficient execution of structured language model programs. *Advances in neural information processing systems*, 37:62557–62583.

Denny Zhou, Nathanael Schärli, Le Hou, Jason Wei, Nathan Scales, Xuezhi Wang, Dale Schuurmans, Claire Cui, Olivier Bousquet, Quoc Le, and 1 others. 2022. Least-to-most prompting enables complex reasoning in large language models. *arXiv preprint arXiv:2205.10625*.

Yinan Zhou, Yuxin Chen, Haokun Lin, Yichen Wu, Shuyu Yang, Zhongang Qi, Chen Ma, and Li Zhu. 2025a. Dogr: Towards versatile visual document grounding and referring. In *Proceedings of the IEEE/CVF International Conference on Computer Vision*, pages 3596–3606.

Yinan Zhou, Yaxiong Wang, Haokun Lin, Chen Ma, Li Zhu, and Zhedong Zheng. 2025b. Scale up composed image retrieval learning via modification text generation. *IEEE Transactions on Multimedia*.

Jiaru Zou, Yikun Ban, Zihao Li, Yunzhe Qi, Ruizhong Qiu, Ling Yang, and Jingrui He. 2025a. Transformer copilot: Learning from the mistake log in LLM fine-tuning. In *Advances in Neural Information Processing Systems 38*.

Jiaru Zou, Xiyuan Yang, Ruizhong Qiu, Gaotang Li, Katherine Tieu, Pan Lu, Ke Shen, Hanghang Tong, Yejin Choi, Jingrui He, James Zou, Mengdi Wang, and Ling Yang. 2025b. Latent collaboration in multi-agent systems. *arXiv preprint*.

A Appendix

A.1 Proof of Theorems in Sec. 4.1

Consider a mini-batch of size G, indexed by $i \in \{1, \dots, G\}$. Each sample has a binary label $Y_i \in \{0, 1\}$. We assume conditional independence given latent Bernoulli parameters:

$$Y_i \mid q_i^\star \sim \text{Bernoulli}(q_i^\star),$$

We assume $\{Y_i\}_{i=1}^G$ are independent given $\{q_i^\star\}_{i=1}^G$. Here $q_i^\star := \mathbb{P}(Y_i = 1 \mid X_i)$ is the true posterior. We have an estimated posterior q_i satisfying a uniform accuracy condition

$$|q_i - q_i^\star| \le \epsilon, \quad \forall i.$$

For any index j, define the *true expected* positive ratio after removing j:

$$\mu_{-j}^\star := \frac{1}{G-1} \sum_{i \neq j} q_i^\star.$$

Likewise define the *estimated* ratio based on $\{q_i\}$:

$$\mu_{-j} := \frac{1}{G-1} \sum_{i \neq j} q_i.$$

We consider the posterior-guided pruning rule

$$\hat{j} := \arg\min_{j \in [G]} |\mu_{-j} - \rho|,$$

where $\rho \in [0, 1]$ is a fixed ratio.

Lemma A.1 (Posterior error transfers to batch ratio)**.** *Given $|q_i - q_i^\star| \le \epsilon$, $\forall i$, for any j, we have*

$$|\mu_{-j} - \mu_{-j}^\star| \le \epsilon.$$

Proof.

$$\begin{aligned} |\mu_{-j} - \mu_{-j}^\star| &= \Big| \frac{1}{G-1} \sum_{i \neq j} (q_i - q_i^\star) \Big| \\ &\le \frac{1}{G-1} \sum_{i \neq j} |q_i - q_i^\star| \\ &= \frac{1}{G-1} (G-1)\epsilon \le \epsilon. \end{aligned}$$

□

Lemma A.2 (Near-optimality of posterior-guided pruning)**.** *Let $j^\star := \arg\min_j |\mu_{-j}^\star - \rho|$ be the best (oracle) removal index. Then given $|q_i - q_i^\star| \le \epsilon$, $\forall i$, we have*

$$|\mu_{-\hat{j}}^\star - \rho| \le \min_j |\mu_{-j}^\star - \rho| + 2\epsilon = |\mu_{-j^\star}^\star - \rho| + 2\epsilon.$$

Proof. By triangle inequality and Lemma A.1,

$$\begin{aligned} |\mu_{-\hat{j}}^\star - \rho| &\le |\mu_{-\hat{j}} - \rho| + |\mu_{-\hat{j}} - \mu_{-\hat{j}}^\star| \\ &\le |\mu_{-\hat{j}} - \rho| + \epsilon. \end{aligned}$$

Since $\hat{j} = \arg\min_j |\mu_{-j} - \rho|$,

$$\begin{aligned} |\mu_{-\hat{j}} - \rho| &\le |\mu_{-j^\star} - \rho| \\ &\le |\mu_{-j^\star}^\star - \rho| + |\mu_{-j^\star} - \mu_{-j^\star}^\star| \\ &\le |\mu_{-j^\star}^\star - \rho| + \epsilon. \end{aligned}$$

Then we have $|\mu_{-\hat{j}}^\star - \rho| \le |\mu_{-j^\star}^\star - \rho| + 2\epsilon$. □

Lemma A.3 (Concentration of realized ratio around its expectation)**.** *Let $\hat{p}_{-\hat{j}} := \frac{1}{G-1} \sum_{i \neq \hat{j}} Y_i$, $\mu_{-\hat{j}}^\star := \frac{1}{G-1} \sum_{i \neq \hat{j}} q_i^\star$, where $Y_i \mid q_i^\star \sim \text{Bernoulli}(q_i^\star)$ are conditionally independent. Then for any $t > 0$,*

$$P\Big(\big| \hat{p}_{-\hat{j}} - \mu_{-\hat{j}}^\star \big| \ge t \,\Big|\, \{q_i^\star\} \Big) \le 2 \exp\big(-2(G-1)t^2 \big).$$

Proof. Condition on the latent parameters $\{q_i^\star\}_{i=1}^G$. Further condition on the (possibly data-dependent) pruned index $\hat{j}$. Given $\hat{j} = j$, the kept labels $\{Y_i\}_{i \neq j}$ remain independent Bernoulli random variables with means $\mathbb{E}[Y_i \mid \{q_k^\star\}, \hat{j} = j] = q_i^\star$ for all $i \neq j$. Define centered variables $Z_i := Y_i - q_i^\star$ for $i \neq j$. Then $\{Z_i\}_{i \neq j}$ are independent, satisfy $\mathbb{E}[Z_i \mid \{q_k^\star\}, \hat{j} = j] = 0$, and are bounded. Since $Y_i \in \{0, 1\}$ and $q_i^\star \in [0, 1]$,

$$Z_i \in [-q_i^\star,\, 1 - q_i^\star] \subseteq [-1, 1].$$

Additionally, we have

$$\hat{p}_{-j} - \mu_{-j}^\star = \frac{1}{G-1} \sum_{i \neq j} (Y_i - q_i^\star) = \frac{1}{G-1} \sum_{i \neq j} Z_i.$$

By Hoeffding's inequality (Hoeffding, 1963), for any $t > 0$, we have

$$\begin{aligned} &P\Big(\hat{p}_{-j} - \mu_{-j}^\star \ge t \,\Big|\, \{q_k^\star\}, \hat{j} = j \Big) \\ \le &\exp\Big(- \frac{2(G-1)^2 t^2}{\sum_{i \neq j} (1 - (-1))^2} \Big) \\ = &\exp\big(-2(G-1)t^2 \big). \end{aligned}$$

Applying the same bound to $-(\hat{p}_{-j} - \mu_{-j}^\star)$ and taking a union bound yields

$$\begin{aligned} &P\Big(\big| \hat{p}_{-j} - \mu_{-j}^\star \big| \ge t \,\Big|\, \{q_k^\star\}, \hat{j} = j \Big) \\ &\le 2 \exp\big(-2(G-1)t^2 \big). \end{aligned}$$

Finally, remove the conditioning on $\hat{\jmath}$:

$$
\begin{aligned}
&P\Big(\big|\hat{p}_{-\hat{\jmath}} - \mu^{\star}_{-\hat{\jmath}}\big| \geq t \;\Big|\; \{q_k^{\star}\}\Big) \\
=&\sum_{j=1}^{G} P(\hat{\jmath} = j \mid \{q_k^{\star}\}) \cdot \\
&\qquad P\Big(\big|\hat{p}_{-j} - \mu^{\star}_{-j}\big| \geq t \;\Big|\; \{q_k^{\star}\}, \hat{\jmath} = j\Big) \\
\leq& 2\exp\big(-2(G-1)t^2\big).
\end{aligned}
$$

□

Theorem 4.2 (High-probability closeness to target ρ.) *Fix $\delta \in (0,1)$. Given $|q_i - q_i^{\star}| \leq \epsilon$, $\forall i$, with probability at least $1-\delta$, we have*

$$
\big|\hat{p}_{-\hat{\jmath}} - \rho\big| \;\leq\; \min_j |\mu^{\star}_{-j} - \rho| \;+\; 2\epsilon \;+\; \sqrt{\frac{\log(2/\delta)}{2(G-1)}}.
$$

Proof. By triangle inequality, we have

$$
|\hat{p}_{-\hat{\jmath}} - \rho| \leq |\hat{p}_{-\hat{\jmath}} - \mu^{\star}_{-\hat{\jmath}}| + |\mu^{\star}_{-\hat{\jmath}} - \rho|.
$$

Use Lemma A.3 with $t = \sqrt{\frac{\log(2/\delta)}{2(G-1)}}$ and Lemma A.2, we can obtain the theorem. □

A.2 Additional Experiment

Effect of Cold-start Steps under Limited Training Budget. In our main experiments, we use 20 cold-start steps to initialize the quality head and pruning estimator. Notably, this cold-start period accounts for less than 5% of the total training process under our original training setting, and is therefore negligible in practice. To further evaluate the effectiveness of ARRoL under limited training budgets, we reduce the maximum training steps to 50 and vary the number of cold-start steps on the Qwen3-1.7B-Base model. The results are shown in Table 7. We observe that removing cold-start entirely (0 steps) leads to a performance drop compared with the baseline GRPO. In contrast, ARRoL remains effective even with a very small cold-start budget, e.g., 5 steps, which corresponds to only 10% of the total training budget.

Table 7: Effect of cold-start steps under a limited training budget. We set the maximum training steps to 50 and evaluate on Qwen3-1.7B-Base. "Baseline" denotes vanilla GRPO without ARRoL.

Cold-start steps	**0**	**5**	**20**	**Baseline**
OlympiadBench	27.15	29.56	29.86	29.26

A.3 Additional Related Work

Efficient Large Language Models. With the advancement in machine learning (Xu et al., 2024a; Zeng et al., 2025c,d, 2026; Wei et al., 2025; Yan et al., 2021a,b, 2024a,b,c; Xia et al., 2025) and foundation models (Zhou et al., 2025b,a; Zhang et al., 2025b; Qiu et al., 2022; Wei et al., 2026b,a; Bei et al., 2026; Liu et al., 2025b; Liu and Yan, 2026), large language models (LLMs) have demonstrated significant potential across various domains, including mathematics (Li et al., 2025), coding (Zou et al., 2025b,a), question answering (Chen et al., 2026a), complex reasoning (Wei et al., 2026a), recommendation (Yoo et al., 2024, 2025a,b; Ban et al., 2023; Yan et al., 2022, 2025), and multi-modality (Bao et al., 2025; Zeng et al., 2026). However, as the number of parameters grows, efficiency becomes a primary bottleneck for practical applications and deployment (Wan et al., 2023; Lin et al., 2026; Chen et al., 2026b). To address this, various methods have been proposed to accelerate both training and inference. Efficient training methods primarily include Parameter-Efficient Fine-Tuning techniques such as LoRA and its variants (Hu et al., 2022; Ding et al., 2023; Wu et al., 2025; Zeng et al., 2025a; Qiu et al., 2026b), low-bit quantization (Dettmers et al., 2023), and memory-efficient strategies like gradient checkpointing and 3D parallelism. Efficient inference methods focus on reducing computational costs through techniques such as post-training quantization (Frantar et al., 2022; Lin et al., 2024b, 2025a; Yang et al., 2025; Bartan et al., 2025; Zhang et al., 2026), structural and non-structural pruning (Lin et al., 2024a; Xing et al., 2025; Ai et al., 2025), and knowledge distillation (Gou et al., 2021) from larger teacher models. Furthermore, specialized LLM inference frameworks have been developed to optimize deployment; for instance, vLLM (Kwon et al., 2023) introduces PagedAttention to manage KV cache memory, while SGLang (Zheng et al., 2024) further optimizes complex LLM programs via the RadixAttention mechanism.

Reasoning in LLMs. Reasoning has evolved from early symbolic AI and graph-based paradigms (He et al., 2026; Xu et al., 2024b; Qiu et al., 2023) such as Knowledge Graph Reasoning (KGR) (Liu et al., 2024), to modern transformer-based architectures (Vaswani et al., 2017; Zeng et al., 2025a,b). While early neural

methods utilized GNNs (Zeng et al., 2023a,b, 2024a,b; Yu et al., 2025b,a; Qiu et al., 2026a, 2024a) to bridge structured data with vector representations, the LLM era has shifted focus toward emergent reasoning through Chain-of-Thought (CoT) prompting (Dou et al., 2025). Recent advancements further enhance these capabilities via post-training reinforcement learning, employing techniques with RLVR, like GRPO (Shao et al., 2024), Dr.GRPO (Liu et al., 2025c), and DAPO (Yu et al., 2025c). These methods move beyond simple next-token prediction by utilizing verifiable rewards to encourage multi-step exploration and self-correction, enabling models to solve complex logical and mathematical problems more reliably.

A.4 Details of Calibration Mapping and Survival Probability Design

As stated in Sec. 4.2, in practice, our quality head outputs an uncalibrated scalar *quality score* s_i for each rollout. We first normalize the score to $s_i \in [0, 1]$ using sigmoid function. We therefore require a calibration mapping $q(s') = P(Y = 1|s'_i)$ to convert scores into posterior estimates. We design an online binned probability calibration.

We employ an estimator with B bins. Specifically, we map a score s' to a bin index $b(s') = \min(B - 1, \lfloor Bs' \rfloor)$. We maintain two labeled buffers of historical rollouts (positive/negative outcomes) and compute histogram counts

$$\begin{aligned} c_b^+ &= \#\{k : b(s_k^+) = b\}, \\ c_b^- &= \#\{k : b(s_k^-) = b\}. \end{aligned} \tag{1}$$

To avoid the situation where $c_b^{+/-} = 0$ in some bins and reduce few-sample noise, we further utilize Laplace smoothing α, and estimate the class-conditional likelihoods:

$$P(b|Y = 1) = (c_b^+ + \alpha)/(\sum_{b' \in [B]} c_{b'}^+ + \alpha B),$$

$$P(b|Y = 0) = (c_b^- + \alpha)/(\sum_{b' \in [B]} c_{b'}^- + \alpha B).$$

Given a prior $\pi = P(Y = 1)$ (estimated from the buffers), we compute posterior-mean estimates via Bayes' rule:

$$\begin{aligned} &q(s) = P(Y = 1 \mid b(s)) \\ &= \frac{\pi P(b(s) \mid Y = 1)}{\pi P(b(s) \mid Y = 1) + (1 - \pi) P(b(s) \mid Y = 0)}. \end{aligned}$$

Based on $q_i = P(Y = 1|s_i)$, we assign each rollout a survival probability using an affine function of the deviation from ρ:

$$p_i = \text{clip}(\kappa + \delta + \lambda(\rho - q_i), p_{\min}, p_{\max}), \tag{2}$$

where κ is the target keep rate, λ controls the strength of balance correction, and δ is a scalar bias. The design goal is: (i) the expected keep ratio matches a target κ, and (ii) the kept rollouts have a controlled positive ratio close to ρ. We solve for δ by binary search such that the expected keep rate matches κ under the current buffer distribution: $\mathbb{E}[p_i] = \kappa$. Finally, clipping to $[p_{\min}, p_{\max}]$ prevents overly aggressive pruning and ensures every rollout retains a non-zero chance to survive, preserving exploration diversity.

In practice, we use $\lambda = 0.5$, $B = 128$.

A.5 Algorithm Framework

Here we present an algorithm framework to better illustrate our system containing fronend and backend, as shown Algorithm 1.

A.6 Potential Risks

We only use public data, and we do not expect any personally identifying information. Our method reduces the cost of RL training, which could lower the barrier to scaling RL-based post-training and be misapplied outside math. We recommend standard safety policies and dataset hygiene when transferring to other domains.

A.7 Declaration of AI Assistance

We used AI tools solely for language polishing. These tools did not contribute to the experiments, analysis, results, or scientific claims, and no paragraphs were generated by AI.

Algorithm 1 ARRoL System

Require: Dataset $\{(x_i, a_i)\}_i$, batch size B, group size G

FRONTEND (verl)

for training step $t = 1, 2, \ldots$ **do**
  Sample prompts $\{(x_i, a_i)\}_{i=1}^{B}$ and form $B \times G$ rollout requests $\mathcal{P}$
  Compute histogram params h_t (binned estimator in Eq. (1), Eq. (2))
  Stream current policy + quality-head weights to backend
  Send $(\mathcal{P}, h_t)$ to backend and wait for responses $\mathcal{R}$ (with prune flags)
  Filter pruned rollouts $\mathcal{R} \to \mathcal{R}'$, rebatch
  Compute rewards, log-probs on $\mathcal{R}'$; main RL loss + quality-head loss
  Backprop and optimizer step on policy and quality head
end for

BACKEND (vLLM)

while requests arrive **do**
  Receive (weights stream, $\mathcal{P}, h$); load/attach weights
  Insert $\mathcal{P}$ into request pool
  while request pool not empty **do**
    Adaptively pick a micro-batch $\{r_i\}_{i=1}^{B'}$ from the pool
    Do one forward step (prefill/decoding) to get next tokens and quality logits
    for each r_i in the micro-batch **do**
      if r_i hits L_{detect} for the first time **then**
        Compute count s_i and survival prob p_i (Eq. (1), Eq. (2))
        Prune r_i w.p. $1 - p_i$; record prune flag
      end if
      Remove completed/pruned requests from pool; mark prune flags
    end for
  end while
  Return all responses (with prune flags) to frontend
end while